

# Combined clarification and affinity capture using magnetic resin enables efficient separation of rAAV5 from cell lysate

Federico Turco,<sup>1,2,3</sup> Adam Wegelius,<sup>1,2,3</sup> Ola Lind,<sup>1</sup> Nils Norrman,<sup>1</sup> Ann-Christin Magnusson,<sup>1</sup> Christine Sund-Lundström,<sup>1</sup> Björn Norén,<sup>1</sup> Jesper Hedberg,<sup>2</sup> and Ronnie Palmgren<sup>1</sup>

<sup>1</sup>Cytiva, Björkgatan 30, 753 23 Uppsala, Sweden; <sup>2</sup>Testa Center, Björkgatan 30, 753 23 Uppsala, Sweden

**Recombinant adeno-associated virus (rAAV) vectors have displayed enormous potential as a platform for delivery of gene therapies. Purification of rAAV at industrial scale involves a series of elaborate, material, and time-consuming midstream steps, such as clarification by depth filtration and concentration/buffer exchange by tangential flow filtration. In this study, we developed a filter-less flow capture method for purification of rAAV serotype 5, using a high-gradient magnetic separator and magnetic Mag Sepharose beads coupled to an AVB affinity ligand. In under 2 h, we captured and eluted rAAV5 directly from ~5 L of cell lysate with a recovery yield of 63% (±5%, n = 3). Compared to cell lysate, the eluate showed a 3-log reduction of host cell DNA and host cell proteins. The process developed eliminates the need for filtration and column chromatography in the early steps of industrial rAAV purification. This will be of high value for industrial-scale manufacturing of rAAVs by reducing time and material in the purification process, without compromising product recovery and purity.**

## INTRODUCTION

Cell and gene therapies hold big promise for treatment of patients, and the FDA predicted that by 2025, up to 20 new cell and gene therapies will be approved each year.<sup>1</sup> One of the most promising cell and gene therapy technologies relies on the use of recombinant adeno-associated virus (rAAV) vectors for the delivery of therapeutics. Clinical trials have been ongoing for several rAAV-related therapies, and to date, five rAAV-based drugs have been launched, being Luxturna, Zolgensma, Glybera, Roctavian, and Upstaza.<sup>2–4</sup> AAV serotype 5 (AAV5) is a promising candidate for gene therapy because of the relative low level of neutralizing antibodies compared to other serotypes<sup>5</sup> and its high cell tropism, which gives AAV5 the ability to target multiple tissues.<sup>6</sup> As the demand for rAAV material is rapidly shifting from bench-scale volumes to high-volume commercial scale, there is an urgent need for fast and scalable production processes to meet expectations in terms of capacity, yield, and quality.<sup>1</sup>

Industrial-scale rAAV production and purification processes can be divided into three main steps: upstream process (USP), midstream process (MSP), and downstream process (DSP) (Figure 1A). Firstly,

during USP, a suitable expression platform such as HEK293T is subjected to a transient triple plasmid transfection for production of the rAAV.<sup>7</sup> MSP begins with lysis of the cells to release the rAAV particles into the medium and is followed by nuclease treatment, clarification of the cell lysate by depth filtration, and concentration/buffer exchange by tangential flow filtration (TFF). In DSP, the filtered material is further processed to obtain purified AAV. The workhorse for capture purification of rAAVs in larger scales is affinity chromatography, which has the objective to selectively purify the required viral vector while simultaneously reducing impurities such as host cell DNA and host cell proteins (HCPs).<sup>8</sup> AVB Sepharose HP, Capto AVB (Cytiva, Sweden), and POROS CaptureSelect (Thermo Fisher Scientific, United States) resins are three of the most popular products on the market for affinity chromatography purification of rAAVs. AVB-coupled resins are made of a base matrix (beads) of agarose coupled with an AVB ligand that has high affinity for AAV1, 2, 3, 5, 6, and rh10.<sup>9</sup> Binding capacities for this resin vary depending on the AAV serotypes, ranging from 10<sup>12</sup> viral particles per mL (VP/mL) (AAV2) to 10<sup>14</sup> VP/mL (AAV5). POROS CaptureSelect AAV8 and AAV9 have shown high affinity for serotypes 8 and 9 respectively,<sup>9</sup> while POROS CaptureSelect AAVX exhibited high affinity for a wide range of serotypes.<sup>10,11</sup> Despite having high binding capacity, commercial chromatography resins have the downside of necessitating complex filtration trains prior to column loading. These filtration steps are sometimes characterized by product loss and negatively impact overall productivity due to long processing times.<sup>12</sup> While the yields of clinically graded rAAV vectors are seldomly shared, the overall process recovery over the USP, MSP, and DSP falls in the range of 30%–35%, assuming a recovery of 80% in each step.<sup>13–15</sup> Nevertheless, recovery yields as low as 22% have been reported for the purification process in its whole,<sup>16</sup> with a recovery after affinity capture of 50%–70%.<sup>11,16</sup> Filtration steps have been associated with losses between 25% and 50%.<sup>11</sup> This is likely to be caused by binding of rAAVs to filter surface

Received 27 February 2023; accepted 25 July 2023;  
<https://doi.org/10.1016/j.omtm.2023.07.010>.

<sup>3</sup>These authors contributed equally

**Correspondence:** Ronnie Palmgren, Cytiva, Björkgatan 30, 753 23 Uppsala, Sweden.

**E-mail:** [ronnie.palmgren@cytiva.com](mailto:ronnie.palmgren@cytiva.com)

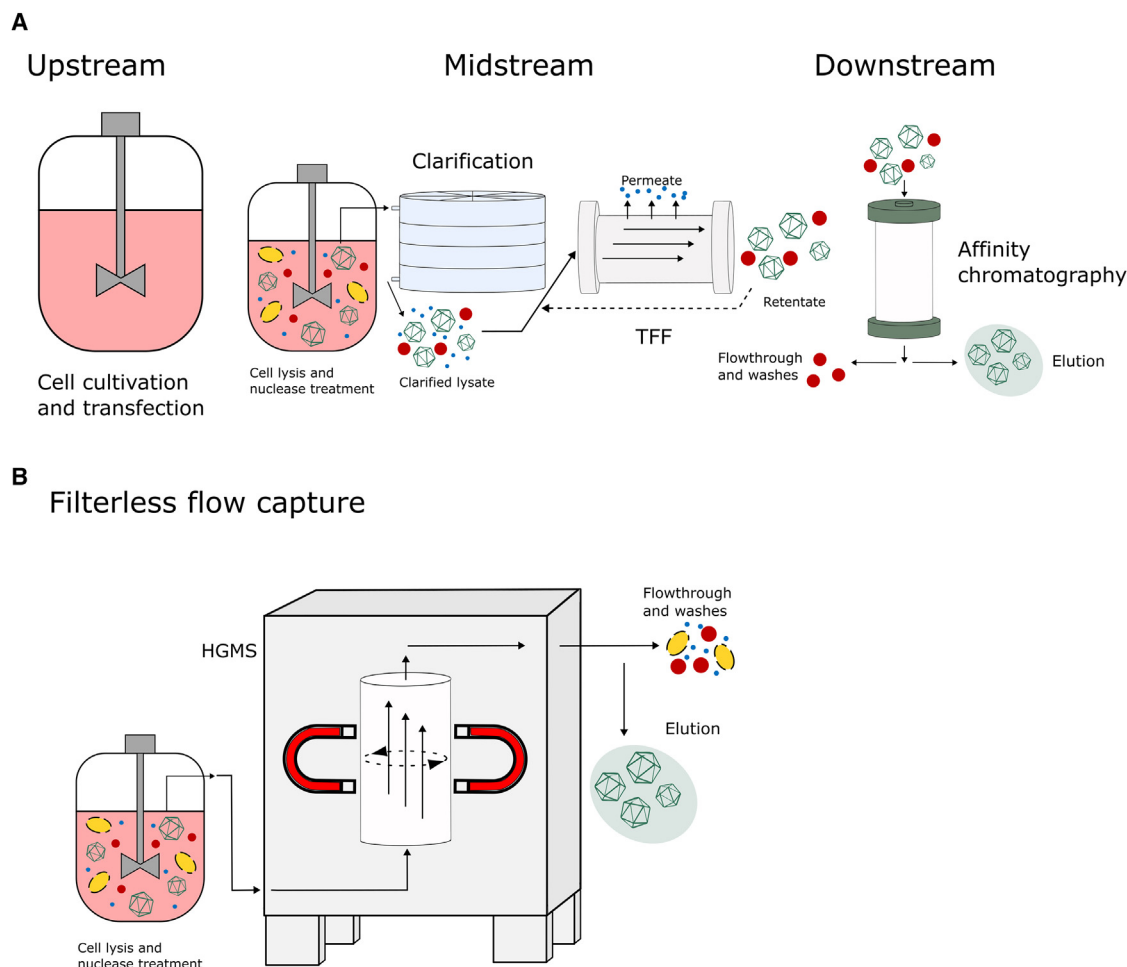


**Figure 1. Overview of rAAV5 production processes**

(A) Typical rAAV industrial production process. During upstream processing, cells are cultivated in a bioreactor and transfected for production of rAAV. During midstream, cells are lysed releasing viral particles (green icosahedrons) and high and low molecular weight impurities (red and blue circles) in the medium. Cell lysate is firstly passed through a series of depth filters for clarification of cell debris (yellow ovals in black dashed lines). Clarified material containing the viral particles, as well as high and low molecular weight impurities, are then subjected to concentration and buffer exchange by tangential flow filtration (TFF). Low molecular weight impurities are removed, while large impurities are retained together with the rAAVs. Eventually, during downstream, TFF retentate is passed through a chromatography column where viral particles are obtained in a bind-elute process. (B) Capture of rAAV5 by means of magnetic separation. Cell lysate is pumped through an HGMS for a single-step direct clarification and capture-elution of viral particles.

and cell debris or by sheer stress, which has been associated with aggregation and inactivation of rAAVs.<sup>11,17–19</sup> Filtration steps are therefore laborious and costly procedures where the need for single-use filtration units, processing time, and loss of viral particles are areas of concern.<sup>11,20,21</sup> Moreover, fouling of filters is sometimes experienced, which further complicates filtration to the disadvantage of product yields and quality.<sup>22</sup>

Magnetic separation has been used for many years in the mining and wastewater industries.<sup>23–25</sup> The concept of magnetic separation applied to the bioprocessing industry involves the use of magnetic chromatography resin that can be used for capture and elution of biotherapeutics directly from the upstream feed. For magnetic processes

to be exploited by the pharmaceutical industry, magnetic particles need to be micron sized with high active surface area, have a distinct magnetic response,<sup>26</sup> and be combined with suitable hardware, capable of generating a strong magnetic field for capturing the magnetic particles. In 2018, a cleanable and sterilizable “rotor stator” high-gradient magnetic separator (HGMS), compliant with GMP-standards, was developed<sup>27</sup> and evaluated for pilot-scale batch purification of mAb (monoclonal antibody) directly from CHO cell culture where an 87.7% yield was obtained with high purity in the eluate.<sup>28</sup> Following, in 2019, Brechman also exploited high-gradient magnetic separators for batch capture of mAbs at the pilot scale.<sup>29</sup> Given the possibility to assimilate clarification and affinity capture in one step, we speculated that magnetic processing would be a promising

**Table 1. Result summary of combined clarification and capture of AAV5 from HEK293T lysate**

Elution volume (after neutralization) (L)	2.3
Eluate titer (VG/mL)	$9.3 (\pm 1.1) \times 10^{10}$
Process yield (%)	63 ( $\pm 5$ )
HCP log reduction	3
dsDNA log reduction	3

Mean values of the three individual experiments are presented. Values within parentheses represent standard deviations.

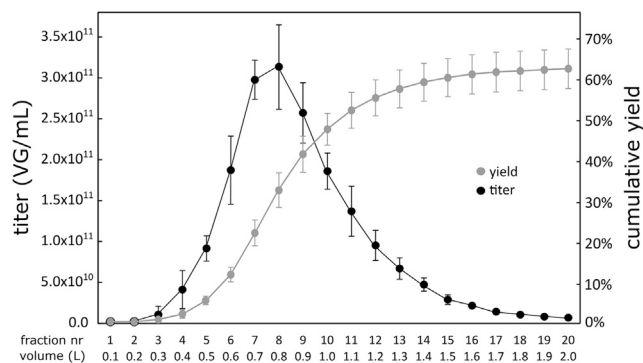
candidate for improvement of the overall process in the demanding manufacturing of rAAVs.

In this study we employed a GMP-graded Andritz HGMS<sup>27</sup> and AVB-coupled Mag Sepharose (AVB Mag Sepharose) beads (Cytiva, Sweden) for affinity capture of rAAV5. The magnetic separator was used in what we describe as a filter-less flow capture mode, originally presented in the patent application by Lind et al. in 2022.<sup>30</sup> In this mode of operation, cell lysate and other process liquids can be continuously flowed through a mixed bed of chromatography resin held in place by a magnetic field. This mode of operation represents a completely novel separation technique with column chromatography-like performance but without the need for clarification of upstream feed prior to column loading.

In this work, we show how crude HEK293T cell lysate can be pumped directly through the stirred bed of AVB Mag Sepharose. Lysed cells and other material pass freely through the bed, while rAAV5 particles are absorbed. The resin slurry is subsequently washed, and the captured rAAV5 particles can be eluted (Figure 1B). Our method is developed to replace the first part of the rAAV5 purification production process, combining clarification and affinity capture in a single step. The results herein presented highlight the potential of this novel magnetic separation approach for a filtration-free, fast, and yield-efficient affinity capture of rAAV5.

## RESULTS

An Andritz HGMS system that allows continuous flow of liquid throughout the separation chamber while simultaneously applying a magnetic field<sup>30</sup> was exploited for filter-less flow capture of rAAV5 directly from cell lysate. A summary of the most important results can be seen in Table 1, whereas a more detailed summary of result and parameters are included in Table S1. Capture of rAAV5 was performed from circa 4.7 L cell lysate from three different cultivations of HEK293T (replicates 1, 2, and 3), obtained by growing, transfecting, and lysing HEK293T cells. Lysates were assessed to have 4.7, 4.9, and  $3.5 \times 10^{11}$  VP/mL respectively for replicates 1, 2, and 3. Viral genome titers for the same lysates were determined by means of qPCR to 7.0, 7.4, and  $7.7 \times 10^{10}$  VG/mL respectively, yielding a proportion of full capsids ranging from 15% (replicate 1 and 2) to 22% (replicate 3) (Table S1). The elution profiles displayed

**Figure 2. Elution peak and cumulative yield of the filter-less flow capture of rAAV5 directly from HEK293T cell lysate**

The elution peak and cumulative yield are represented by black and gray circles respectively. The elution peak was determined by measuring the viral titer (VG/mL, left Y axis) in each elution fraction. The cumulative yield is reported as percentage of the total VG recovered (right Y axis) in the eluate fractions in relation to the total VG content in the upstream HEK293T cell lysate. The X axis reports the number of fraction and the cumulative volume. Data points represent means of three individual experiments. Error bars represent standard deviation.

near-Gaussian peak shapes and showed that the rAAV5 could be eluted in around 2 L of elution buffer (Figure 2 and Table 1). Viral genome titer in the eluates were determined to  $8.3 \times 10^{10}$ ,  $9.1 \times 10^{10}$ , and  $1.1 \times 10^{11}$  VG/mL, representing an average yield of 63% ( $\pm 5$ ) (Figure 2 and Table 1). On average between the three runs, 3% of the total loaded viral genomes were found in both the flow-through and wash fractions. For replicates 1 and 3, elution fraction numbers 4–14 (Figure 2) were pooled and average viral particle titer assessed to  $8.4 (\pm 3.8) \times 10^{11}$  VP/mL, with an average proportion of full particles of 21% ( $\pm 6$ ) (Table S1). Processing of 4.7 L of cell lysate required 6 L of equilibration buffer to equilibrate 400 mL of magnetic resin and to perform the first washing step, 4 L of H<sub>2</sub>O to wash the separation chamber prior to elution, and 2 L of elution buffer. Individual runs took less than 2 h to complete, excluding buffer preparation and post-run cleaning.

Levels of double-stranded DNA (dsDNA, used as a measure of host cell DNA) and HCP were analyzed in the cell lysate and eluate fractions of the experimental replicates (Figure 3A). Concentration of dsDNA measured by PicoGreen assay showed a 3-log reduction between the lysate and the eluate (Figure 3A and Table S1). Concentration of HCP, measured by means of HEK293 HCP immunoassay kit for Gyrolab, was below level of quantification (LoQ, 7.8 ng/mL) in eluates from replicates 1 and 2, whereas eluate from replicate 3 contained around 44 ng HCP/mL. A 3-log reduction of HCP between the lysate and the eluate could be confirmed for all three replicates (Figure 3A and Table S1).

A representative western blot against AAV capsid proteins in the eluate and cell lysate can be seen in Figure 3B. Total protein pre-staining with Cy5<sup>31</sup> was used to visualize total protein content, while viral proteins were detected using a primary antibody and a Cy3-labeled

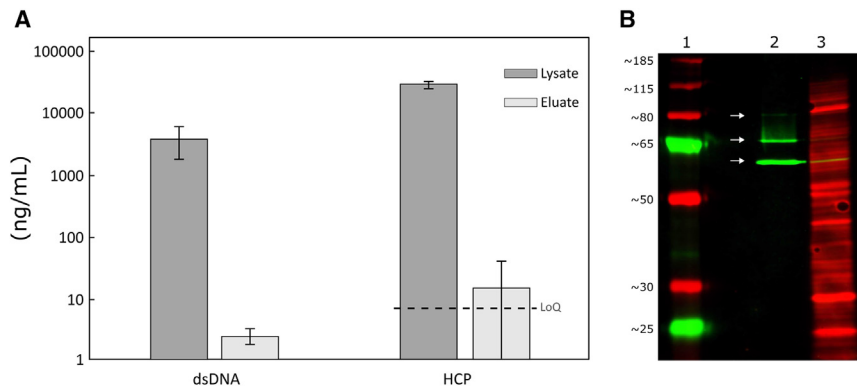


**Figure 3. Impurity analysis of the eluate from the filter-less flow capture of rAAV5 directly from HEK293T cell lysate**

(A) Concentration of dsDNA and HCP in the lysate (dark gray bars) and eluate (light gray bars plotted on a logarithmic scale). For the HCP, the limit of quantification (LoQ = 7.8) is reported as a black dashed line. Bars represent means of three individual experiments, and error bars represent standard deviation. In the case of HCP, two out of three replicates were below the LoQ. For these replicates, since no accurate datapoint could be acquired, the LoQ value was used to calculate the mean. For details regarding the individual measurements, see [Table S1](#). (B) Representative western blot against AAV capsid proteins targeted with Cy3-labeled secondary antibody in the

eluate (lane 2) and cell lysate (lane 3), with total protein pre-staining using Cy5 dye. Figure depicts overlay image of the two channels, with the Cy3 signal colored green and the Cy5 signal colored red. White arrows indicate positions of the three bands corresponding to viral capsid proteins VP1, 2, and 3. Lane 1 displays a protein ladder for approximate size determination. Numbers next to the ladder represent approximate molecular weights in kDa.

secondary antibody. [Figure 3B](#) also shows an overlay of the AAV5-specific (green) and total protein (red) signals. Non-overlaid signals are displayed in [Figure S1](#). Western blotting revealed two clear bands in the eluate, corresponding to the size of the viral capsid proteins VP2 and VP3 (72 kDa and 62 kDa respectively<sup>32</sup>). A less pronounced band was revealed at a higher molecular weight, corresponding to the size of the viral capsid protein VP1 (87 kDa<sup>32</sup>). Bands corresponding to viral capsid proteins could be detected also in the cell lysate (lane 3, [Figures 3B](#) and [S1A](#)). Cy5 total protein staining failed to reveal any significant protein impurities in the elution fraction (lane 2, [Figures 3B](#) and [S1B](#)).

## DISCUSSION

The current state-of-the-art production pipeline for rAAVs includes complex and time-consuming, midstream filtration steps, followed by affinity chromatography purification.<sup>9</sup> As the process is characterized by loss of viral particles and low productivity,<sup>11</sup> development of efficient, easy-to-perform, and scalable purification procedures for rAAVs is pivotal to reduce manufacturing costs and increase availability of important therapies.<sup>9</sup> In this study, we used an Andritz HGMS, loaded with Mag Sepharose magnetic chromatography resin coupled to an AVB ligand for combined clarification and affinity capture of rAAV5 directly from cell lysate. We show a successful affinity capture-and-elute process of rAAV particles without prior filtration of cell lysate, at an industry-relevant scale. The described filter-less flow capture technique yields capture, washing, and elution performance similar to column chromatography. Previous relevant studies where magnetic separation was exploited for the purification of biotherapeutics (exclusively mAbs) either relied entirely on batch processes<sup>28</sup> or on a mixed approach where different containers were used in different steps of the process.<sup>29</sup>

The most striking advantage of our method is the complete removal of clarification and concentration steps prior to affinity capture. Cell lysate can be directly pumped, from any suitable container (preferably the container used for the cell lysis), directly to the affinity resin. The process is quick and does not require chromatographic expertise. A

traditional purification process, starting from lysed and nuclease treated cell material, entails different complex and time-consuming steps. Firstly, acid precipitation is typically used to remove chromatin aggregates and other host cell contaminants.<sup>33</sup> This step is needed to avoid clogging of the clarification filters and takes, in our experience, around 8–12 h (often performed overnight). Second, the cell lysate is clarified by depth filtration and further purified, concentrated, and buffer exchanged by TFF. In a typical process, the feed is then passed through a 0.2- $\mu$ m membrane filter to protect downstream columns and equipment. The total time required to perform the filtration steps is usually around 8 h. From 5 L of cell lysate, around 400 mL of concentrated material is expected after the filtrations. Finally, processing of 400 mL of material in the column chromatography capture step would take around 2 h. Based on this, the overall time required to obtain eluate from the capture step when using a state-of-the-art production process, including precipitation, clarification, TFF, and capture, is around 20 h. On the other hand, when using the magnetic process, we were able to process circa 5 L of cell lysate within 2 h, and the process involves no packed chromatography column. Prior to the run, magnetic beads were simply pumped into the magnetic chamber and retained by the magnetic field. Processing 5 L of cell lysate with a viral titer of  $4.7 \times 10^{11}$  VP/mL with traditional methodologies involving MSP would result in a productivity of  $1.2 \times 10^{14}$  VP/hour, accounting for the 20-h total processing time. However, by exploiting the technique herein developed, the productivity would be  $1.2 \times 10^{15}$  VP/hour (2-h processing time), corresponding to a 1-log increase.

By using the filter-less flow affinity capture described here, it was possible to purify rAAV5 from 4.7 L of cell lysate, achieving an overall recovery yield of ~63% measured in relation to upstream feed (by means of qPCR). The rAAV5 was eluted in one peak with a near-Gaussian shape with circa 2 L of elution buffer ([Figure 2](#)). The levels of HCP and dsDNA measured in our eluate showed 3-log reduction in relation to cell lysate ([Figure 3A](#) and [Table S1](#)). Western blot with total protein staining ([Figure 3B](#)) confirmed the presence of the viral capsid proteins in the eluate and revealed no protein impurities or degradation products. This, together with titer, HCP, and dsDNA

data, suggests that the eluate had intact viral particles and low levels of impurities. In a recent publication, critical process parameters such as recovery yields and reduction of impurities were assessed for an industrial “gold standard” rAAV5 production process throughout MSP and DSP.<sup>21</sup> In this study,  $57\% \pm 30\%$  of rAAV5 viral genomes was recovered after affinity chromatography purification, while a 3-log and 1.5-log reduction in the concentration of HCP and dsDNA was observed in the eluate.<sup>21</sup> The new methodology presented in this work compares well in terms of recovery yield and reduction of impurities, but it outperforms current industrial state of the art in respect to processing time and productivity. As described, we used Mag Sepharose functionalized with the AVB ligand. However, as Mag Sepharose can be functionalized with any ligand as readily as standard Sepharose beads, the technique presented here could easily be implemented for other processes.

Filtration steps during midstream are characterized by losses between 25% and 50%.<sup>11</sup> These losses were not converted in gains with the combined clarification and affinity capture step herein described despite elimination of filtration procedures. As only minimal loss of viral particles was detected in the flowthrough (circa 3%, [Table S1](#)), we speculate this is likely to be due to viral particles binding to various inert surfaces and/or sticking to cell debris as previously reported elsewhere.<sup>11,17,19,34</sup>

An advantage of using AVB-coupled resin is the possibility to directly load the eluate on IEX (ion-exchange chromatography) columns for enrichment of full capsids. The elution of the viral particles, as reported here, is carried out with 50 mM glycine (pH 2.5). The eluate is thereafter neutralized to pH 9 using a small volume of 200 mM tris base (pH 10). The low conductivity and high pH of the eluate are ideal conditions for direct continuation of the process with separation of full and empty capsids by means of anion exchange chromatography resins such as Capto Q (Cytiva, Sweden).<sup>35,36</sup> Using the direct filter-less flow capture procedures reported here, it is therefore possible to achieve enrichment of full capsids within hours of completed cell lysis. Furthermore, AVB Mag Sepharose particles can be subjected to cleaning in place (CIP) per instruction for commercially available AVB Sepharose chromatography resins. CIP is pivotal to yield high-quality products and reduce process cost by allowing multiple purifications in series using the same resin.<sup>28</sup> In this work, the same AVB Mag Sepharose resin was used for all replicates, and CIP procedure was performed in between each experiment without loss of performance. Reusability of affinity chromatography resins depends on the coupling chemistry and the ligand attached to the base matrix. As commercial non-magnetic AVB resins (AVB Sepharose and Capto AVB) have the same ligand and coupling chemistry as the magnetic resin used in this study, CIP procedures remain unaffected, and AVB Sepharose resins can be reused several times.

One notable difference between direct filter-less flow capture of rAAV, as described in this work, and more traditional approaches is the elution volume. The total elution volume of around 2 L is a significantly higher volume than you would expect from a conventional MSP-DSP

approach, where a small volume of TFF-concentrated sample is loaded on a relatively small affinity capture column. This is important to note, and the significance of this difference will depend on the steps further downstream in the process. In our experience, a suitable concentration of the product is easily achievable in the downstream separation of full and empty capsids using IEX chromatography, or otherwise in buffer exchange steps prior to formulation. Therefore, the increased volume from the capture step does not have to be a significant drawback. However, this will ultimately have to be evaluated in the individual processes where our methodology would be considered.

While eliminating the need for complicated filtrations steps resulted in increased productivity, additional optimization of different parameters of the combined clarification and affinity capture process may result in further improvements. Firstly, one of the main aspects to consider when developing industrial processes is scalability. In this pilot study, we processed approximately 5 L of cell lysate in commercially available Andritz HGMS having a separation chamber of 1 L. The process is partially scalable as the same HGMS is available with a 10 L separation chamber, thereby allowing the processing of 10 times more cell lysate in the same time frame. Nevertheless, 500 L cell lysate is considered a suitable scale for production of AAV for clinical trials. To process such a volume with a 10-L HGMS, a biopharmaceutical manufacturer would either have to perform 10 cycles of bind-elute, which would take approximately 20 h, or use 10 separators in parallel to be able to process the lysate in 2 h. Development of suitable hardware, or major improvements to existing hardware, could facilitate larger volumes of magnetic resin in the separation chamber and enable processing of larger batches. Secondly, the base matrix employed to couple the AVB ligand was originally developed for purification of mAbs. The design of AAV-tailored magnetic resins and increasing density of the ligand on the base matrix may improve binding capacity of the resin and recovery yields, improving overall process economy. Thirdly, flow rates and volumes of buffers used in the different steps of the process were not experimentally determined but rather estimated based on manufacturer recommendations for AVB Sepharose chromatography resins (Cytiva, Sweden). Experimental investigation of these parameters may result in further reduction of processing time and boost productivity. Fourthly, despite that 400 mL of AVB Mag Sepharose was used in this study, a maximum of 480 mL of magnetic particles could have been loaded into the separation chamber of the Andritz system (80% of the maximal magnetic binding capacity),<sup>28</sup> thereby further increasing process efficiency and product concentration. Lastly, maximum viral load on the magnetic AVB resin was not measured. Capacity of the commercially available Capto AVB resin for rAAV5 in filtered material is on the order of  $10^{14}$  VP/mL, whereas we loaded circa  $4.6 \times 10^{12}$  VP/mL of AVB Mag Sepharose resin to ensure full absorption and minimal breakthrough. The reason for the decreased load is the reduced binding capacity of the beads when deployed directly in cell lysate. Batch absorption isotherm experiment showed approximately 2-log lower maximal binding capacity when performed in cell lysate compared to clarified, concentrated, and buffer-exchanged material (data not shown). However, since the purification procedure applied here does not involve batch

absorption, but a continuous flow through the separation chamber, the actual binding capacity may not be accurately determined from batch absorption data. The low concentration of viral particles in our flowthrough (Table S1) may indicate that we are operating below binding capacity. Given sufficient availability of upstream feed, a dynamic binding capacity experiment for the AVB Mag Sepharose particles could be performed to fairly define the real capacity of filter-less flow capture of rAAV5 with the Andritz HGMS and possibly reveal increased capacity of the technique.

In summary, we developed an HGMS-mediated filter-less flow capture process for combined clarification and affinity capture of rAAV5 directly from cell lysate. Our methodology is an attractive alternative to current state-of-the-art procedures due to (1) dramatically reduced processing time and increased productivity, (2) removal of all filters needed during MSP, (3) yields comparable to established industrial processes, (4) satisfactory reduction of dsDNA and HCP, (5) production of eluate that could readily be loaded directly onto an IEX column for further full capsid enrichment, and (6) an easy to use, combined clarification and affinity capture step requiring limited operator training.

Overall, we believe that further optimization of process parameters such as flow rates, exploitation of the full magnetic capacity of the Andritz system, and design of AAV-tailored magnetic base matrix may further improve yields and productivity of our technique. Regardless, considering the short process time and the removal of all filtration steps, we already now put forth the method presented in this work as a way of saving both time and material when purifying rAAVs on a larger scale.

## MATERIALS AND METHODS

### Cell cultivation, rAAV production, and lysis

HEK293T (American Type Culture Collection, United States) cultivation was performed in batch mode, either using a ReadyToProcess WAVE 25 bioreactor system in HyClone HyCell TransFx-H (Cytiva, Sweden) (replicates 1 and 3) or in single-use 5-L baffled polycarbonate Erlenmeyer flasks (Corning, United States) in Gibco FreeStyle 293 Expression Medium (Thermo Fisher Scientific, United States) (replicate 2). Triple plasmid transfection, lysis, and DNase treatment were performed according to procedures established by Cytiva, available online and on request (application note: adeno-associated virus production in suspension HEK293 cells with single-use bioreactors).<sup>37</sup> Plasmids for transfection were purified using ZymoPURE II Plasmid Maxiprep Kit (Zymo Research, United States) according to manufacturer's instruction, including the extra endotoxin removal step. After cell lysis, viral titer was determined, and the lysate was frozen at  $-80\text{ }^{\circ}\text{C}$  for storage until further processing.

### Magnetic particles

For purification of rAAV5, Mag Sepharose was functionalized with the AVB ligand, provided by Cytiva Sweden. Coupling of the ligand to Mag Sepharose was done with NHS activation chemistry. The ligand is attached to the base matrix via a hydrophilic spacer arm to make it easily available for binding of the virus.

### Combined clarification and affinity capture

The one-step combined clarification and capture was performed in a rotor-stator HGMS, MES 100 RS (Andritz, Germany). Two modifications to the Andritz HGMS were introduced in this work: (1) enabling pump and mixing functions while the electromagnet is on<sup>30</sup> and (2) bypassing the automatic valves using silicone tubing and manual clamp valves (Figure S2). The first is essential to operate the system as described in this work and requires technical support from the manufacturer to implement. The second one was implemented by the operators for convenience and is not essential to run the process as described. The first modification enabled us to operate the separator in a filter-less flow mode, where buffers and cell lysate are pumped through the mixed separation chamber with the magnetic particles retained by the magnetic field. For an extensive description of the MES 100 RS in its original configuration, used in a bio-processing context, please refer to Ebeler et al.<sup>28</sup>

The conditions used for the combined clarification and capture are summarized in Table S2. To fill the separator with magnetic particles, a 50% slurry of AVB Mag Sepharose in 20% ethanol was pumped into the separation chamber at 180 mL/min with mixing set at 5% (75 rpm) and the magnet turned on. A total volume of 400 mL AVB Mag Sepharose was placed to the chamber in this way, and no leakage of magnetic particles was observed on the outlet side. Following this, the separation chamber was equilibrated with 4 L AVB binding buffer (20 mM Tris, 0.5 M NaCl, pH 8.5) using the same flowrate and mixing as above.

For loading of rAAV5 particles on AVB Mag Sepharose, thawed cell lysate was pumped through the separation chamber at a pump speed of 92 mL/min with magnet turned on and mixing set at 5% (75 rpm). This corresponds to a residence time of 10.9 min in the separation chamber. In all runs, a total of  $1.6 \times 10^{15}$  viral particles were loaded on the 400 mL AVB Mag Sepharose resulting in a load of  $4 \times 10^{12}$  VP/mL resin. During the loading, flowthrough was collected for rAAV5 concentration determination. After the loading, the separation chamber was washed with 4 L AVB binding buffer and 2 L purified water at 390 mL/min and 15% (225 rpm) stirring. Washing liquids were collected for rAAV concentration determination.

Elution was achieved by pumping 50 mM glycine (pH 2.5) through the chamber at 250 mL/min with the stirring set at 15% (225 rpm). Elution liquid was manually collected in fractions of circa 100 mL, and 8.5 mL of neutralization buffer (200 mM tris base, pH 10) was added to each fraction. In total, 20 fractions from each run were collected and saved for analysis.

Before and after every experimental run, magnetic particles were CIP-ed according to the procedure described in [materials and methods](#), cleaning-in-place, summarized in [Table S3](#).

Calculations of the productivity of the filter-less flow magnetic process and traditional purification process were performed as follows: productivity = ((VP/mL) x volume feed processed)/hours

required to run the process. Therefore, for the traditional and magnetic processes the calculations are, respectively:  $(4.7 \times 10^{11} \text{ VP/mL}) \times 5000 \text{ (mL)}/20 \text{ h} = 1.2 \times 10^{14} \text{ VP/hour}$  and  $(4.7 \times 10^{11} \text{ VP/mL}) \times 5000 \text{ (mL)}/2 \text{ h} = 1.2 \times 10^{15} \text{ VP/mL}$ .

#### Viral titer

The viral genome copies were determined by qPCR using a StepOneSystem, Real-time PCR system (Applied Biosystem, United Kingdom). Samples from the different steps of the process were diluted 1,000x in PBS (Cytiva, Sweden). The reaction mix was composed of a TaqMan universal PCR mastermix (Applied Biosystems), CMV forward primer (TGGAGTTCGCGTTACATAACTT), CMV reverse primer (ACGTTACTATGGGAACATACGTCATT), and CMV probe (6FAM, HPLC, CCTGGCTGACCGCC), all ordered from Thermo Fisher Scientific (United States). Reaction volume was 30  $\mu\text{L}$ , and the qPCR thermocycler was set up with two hold steps, 50°C for 2 min and 95°C for 10 min, followed by 40 cycles of 95°C for 15 s and 60°C for 1 min. Each sample was run in technical duplicates, and the average concentrations were considered if the coefficient of variation was below 15%. The standard curve was prepared from an in-house produced plasmid, linearized prior to the qPCR. An internal reference sample (rAAV5 diafiltration retentate) of known concentration and a recombinant adeno-associated virus 2 VR-1616 (American Type Culture Collection, United States) were used as positive controls. PBS and ddH<sub>2</sub>O, used for the dilutions and preparation of the mastermix, respectively, were employed as negative controls.

Total viral particles were determined using Gyrolab AAVX Titer Kit (Gyros Protein Technologies, Sweden). Experiments were performed on a Gyrolab workstation (Gyros Protein Technologies, Sweden) following kit instructions and recommended dilutions. The standard curve for the run was prepared according to kit instructions, using purified AAV5 capsids with known concentration (AAV5 empty capsids 66V050, Progen, Germany). Data were collected and evaluated using the Gyrolab Evaluator software.

The percentage of full particles was calculated as the ratio between viral genome copies and total viral particles, multiplied by 100.

#### dsDNA

dsDNA concentrations were determined using the Quant-iT PicoGreen dsDNA Assay Kit (Thermo Fisher Scientific, USA). Lysates were diluted 100 times in TE buffer prior to analysis, whereas eluates were analyzed undiluted. Each replicate was measured three times (technical triplicate). For each time TE buffer, standard curve and sample dilution were freshly prepared. The assay was performed according to manufacturer's instructions, and all measurements fell within the recommended standard curve. A fluorescence plate reader (Spectramax Gemini XPS, Molecular Devices, United States) was used to capture fluorescence data at 485/538 nm.

#### Host cell protein

Host cell protein levels were determined using HEK 293 HCP Reagent Set for Gyrolab (Cygnum Technologies, United States) together with a

Gyrolab Bioaffy 1000 HC Assay Toolbox (Gyros Protein Technologies, Sweden). Experiments were performed on a Gyrolab workstation (Gyros Protein Technologies, Sweden) according to kit instructions. Data were collected and evaluated using the Gyrolab Evaluator software. LoQ was determined according to Armbruster and Pry<sup>38</sup> to be 7.8 ng/mL.

#### Western blot with Cy5 total protein staining

Total protein pre-labeling reaction was done with Cy5 total protein stain (Cytiva, Sweden) according to Hagner-McWhirter et al.<sup>31</sup> in a 20- $\mu\text{L}$  reaction volume. Following the pre-labeling reaction, NuPAGE LDS sample buffer and NuPAGE reducing agent (Thermo Fisher Scientific, United States) were added to the sample as prescribed by the manufacturer. Samples were denatured at 70°C for 10 min and subsequently loaded together with a pre-stained page ruler on a NuPAGE 10% Bis-Tris gel (Thermo Fisher Scientific, United States) stacked in a Xcell SureLock Mini Cell (Thermo Fisher Scientific, United States). Blotting was done to an Amersham WB PVDF membrane (Cytiva, Sweden) using an Xcell blot module (Thermo Fisher Scientific, United States). Both SDS-PAGE and transfer were done following manufacturer's instructions and buffer recommendations. Post transfer, the membrane was blocked for 1 h in 3% BSA (bovine serum albumin) (Thermo Fisher Scientific, United States) in PBS with 0.1% Tween 20 (PBS-T) (Thermo Fisher Scientific, United States). After blocking, the membrane was incubated for 2 h with anti-AAV VP1/VP2/VP3 mouse monoclonal antibody (Progen, Germany), diluted 1:100 in blocking buffer, and subsequently washed 4 x 10 min in PBS-T. The membrane was then incubated with Amersham WB goat anti-mouse Cy3-labeled antibody (Cytiva, Sweden), diluted 1:2,500 in PBS-T, for 1 h, and washed as described above. Fluorescence and color images were captured with the Amersham ImageQuant 800 using the SNOW exposure mode and 1 x 1 binning. The grayscale.tiff images were analyzed with ImageQuant TL 10.2 analysis software from Cytiva. **Figure 3B** shows a multi-color overlay image using two images captured with Cy3 (green) and Cy5 (red) LED-filter combinations.

#### DATA AND CODE AVAILABILITY

All data will be made available upon reasonable request.

#### SUPPLEMENTAL INFORMATION

Supplemental information can be found online at <https://doi.org/10.1016/j.omtm.2023.07.010>.

#### ACKNOWLEDGMENTS

We thank Josefin Thelander and Greta Hulting at Cytiva for their kind help and support with cell cultivation, transfection, and impurity analysis. Åsa Hagner-McWhirter and Elin Monie at Cytiva are kindly acknowledged for their assistance with western blotting. We thank Erik Bjerneld at Cytiva for his assistance with image analysis. We thank Åsa Hagner-McWhirter, Nick Westaway, and Anita Solbrand at Cytiva for suggestions on how to improve the manuscript. Finally, we thank the bioprocess specialists at Testa Center, Dimitra Peiras-maki and Louise Fitkin, for their patience and support during the conduction of this study.

## AUTHOR CONTRIBUTIONS

F.T., A.W., A.-C.M., and C.S.-L. produced the rAAV5. B.N. coupled the AVB ligand to Mag Sepharose. F.T., A.W., O.L., and N.N. conceived and planned the experiments. R.P. and J.H. organized and coordinated the work. F.T. and A.W. executed the experiments and wrote the manuscript. O.L., N.N., J.H., and R.P. edited the manuscript.

## DECLARATION OF INTERESTS

All authors are employees of Cytiva Sweden AB, and the majority are named inventors on various patents covering methods and/or equipment related to bioprocessing, chromatography, AAV manufacturing, and/or other similar applications.

## REFERENCES

- Adams, B., Bak, H., and Tustian, A.D. (2020). Moving from the bench towards a large scale, industrial platform process for adeno-associated viral vector purification. *Biotechnol. Bioeng.* *117*, 3199–3211.
- Keeler, A.M., and Flotte, T.R. (2019). Recombinant Adeno-Associated Virus Gene Therapy in Light of Luxturna (and Zolgensma and Glybera): Where Are We, and How Did We Get Here? *Annu. Rev. Virol.* *6*, 601–621.
- European Medicines Agency (2022). Roctavian, medicine overview Roctavian; INN-valoctocogene roxaparvec. [europa.eu](https://www.ema.europa.eu).
- European Medicines Agency (2022). Upstaza, medicine overview Upstaza; INN-eladocicigine exuparvec. [europa.eu](https://www.ema.europa.eu).
- Boutin, S., Monteilh, V., Veron, P., Leborgne, C., Benveniste, O., Montus, M.F., and Masurier, C. (2010). Prevalence of serum IgG and neutralizing factors against adeno-associated virus (AAV) types 1, 2, 5, 6, 8, and 9 in the healthy population: implications for gene therapy using AAV vectors. *Hum. Gene Ther.* *21*, 704–712.
- Aschauer, D.F., Kreuz, S., and Rumpel, S. (2013). Analysis of transduction efficiency, tropism and axonal transport of AAV serotypes 1, 2, 5, 6, 8 and 9 in the mouse brain. *PLoS One* *8*, e76310.
- Kimura, T., Ferran, B., Tsukahara, Y., Shang, Q., Desai, S., Fedoce, A., Pimentel, D.R., Luptak, L., Adachi, T., Ido, Y., et al. (2019). Production of adeno-associated virus vectors for *in vitro* and *in vivo* applications. *Sci. Rep.* *9*, 13601.
- Wright, J.F. (2014). Product-Related Impurities in Clinical-Grade Recombinant AAV Vectors: Characterization and Risk Assessment. *Biomedicines* *2*, 80–97.
- Mietzsch, M., Smith, J.K., Yu, J.C., Banala, V., Emmanuel, S.N., Jose, A., Chipman, P., Bhattacharya, N., McKenna, R., and Agbandje-McKenna, M. (2020). Characterization of AAV-Specific Affinity Ligands: Consequences for Vector Purification and Development Strategies. *Mol. Ther. Methods Clin. Dev.* *19*, 362–373.
- Touelle, M., Dejoint, L., Attebi, E., Cartigny, J., Rasle, C., Potier, S., Rundwasser, S., Guianvarc'h, L., Lebec, C., and Hebben, M. (2018). Development of purification steps for several AAV serotypes using POROS™ CaptureSelect™ AAVX affinity chromatography. *Cell Gene Ther. Insights* *4*, 637–645.
- Florea, M., Nicolaou, F., Pacouret, S., Zinn, E.M., Sanmiguel, J., Andres-Mateos, E., Unzu, C., Wagers, A.J., and Vandenberghe, L.H. (2023). High-efficiency purification of divergent AAV serotypes using AAVX affinity chromatography. *Mol. Ther. Methods Clin. Dev.* *28*, 146–159.
- Zhao, M., Vandersluis, M., Stout, J., Hapts, U., Sanders, M., and Jacquemart, R. (2019). Affinity chromatography for vaccines manufacturing: Finally ready for prime time? *Vaccine* *37*, 5491–5503.
- Hebben, M. (2018). Downstream bioprocessing of AAV vectors: industrial challenges & regulatory requirements. *Cell Gene Ther. Insights* *4*, 131–146.
- Wright, J.F., Le, T., Prado, J., Bahr-Davidson, J., Smith, P.H., Zhen, Z., Sommer, J.M., Pierce, G.F., and Qu, G. (2005). Identification of factors that contribute to recombinant AAV2 particle aggregation and methods to prevent its occurrence during vector purification and formulation. *Mol. Ther.* *12*, 171–178.
- Rashnnejad, A., Chermahini, G.A., Li, S., Ozkinay, F., and Gao, G. (2016). Large-Scale Production of Adeno-Associated Viral Vector Serotype-9 Carrying the Human Survival Motor. *Mol. Biotechnol.* *58*, 30–36.
- Tomono, T., Hirai, Y., Okada, H., Miyagawa, Y., Adachi, K., Sakamoto, S., Kawano, Y., Chono, H., Mineno, J., Ishii, A., et al. (2018). Highly Efficient Ultracentrifugation-free Chromatographic Purification of Recombinant AAV Serotype 9. *Mol. Ther. Methods Clin. Dev.* *11*, 180–190.
- Bennicelli, J., Wright, J.F., Komaromy, A., Jacobs, J.B., Hauck, B., Zelenia, O., Mingozzi, F., Hui, D., Chung, D., Rex, T.S., et al. (2008). Reversal of blindness in animal models of leber congenital amaurosis using optimized AAV2-mediated gene transfer. *Mol. Ther.* *16*, 458–465.
- Morgan, B.A., Manser, M., Jeyanathan, M., Xing, Z., Cranston, E.D., and Thompson, M.R. (2020). Effect of Shear Stresses on Adenovirus Activity and Aggregation during Atomization To Produce Thermally Stable Vaccines by Spray Drying. *ACS Biomater. Sci. Eng.* *6*, 4304–4313.
- Adamson-Small, L., Lundgren, M., and Guterstam, P. (2020). Scalable and efficient AAV production process with new Fibro chromatography technology. *Cell Gene Ther. Insights* *6*, 1249–1262.
- Silva, R.J., Mota, J.P., Peixoto, C., Alves, P.M., and Carrondo, M.J. (2015). Improving the downstream processing of vaccine and gene therapy vectors with continuous chromatography. *Pharm. Bioprocess.* *3*, 489–505.
- Hejmowski, A., Olson, M., MacIntyre, A., Rose, A., Boenning, K., Huato, J., Schofield, M., Kavara, A., Marchand, N., and Collins, M. (2021). Enrichment of full rAAV capsids in a scalable, reproducible viral vector manufacturing platform. *Cell Gene Ther. Insights* *7*, 1563–1579.
- Hongyu, L., and Chen, V. (2010). In Chapter 10 - Membrane Fouling and Cleaning in Food and Bioprocessing. *Membrane Technology*, Z.F. Cui and H.S. Muralidhara, eds., pp. 213–254.
- Dong, T., Yang, L., Zhu, M., Liu, Z., Sun, X., Yu, J., and Liu, H. (2015). Removal of cadmium(II) from wastewater with gas-assisted magnetic separation. *Chem. Eng. J.* *280*, 426–432.
- Franzreb, M., and Holl, W. (2000). Phosphate removal by high-gradient magnetic filtration using permanent magnets. *IEEE Trans. Appl. Supercond.* *10*, 923–926.
- Svoboda, J. (1982). Magnetic flocculation and treatment of fine weakly magnetic minerals. *IEEE Trans. Magn.* *18*, 796–801.
- Tartaj, P., Morales, M.P., González-Carreño, T., Veintemillas-Verdaguer, S., and Serna, C.J. (2005). Advances in magnetic nanoparticles for biotechnology applications. *J. Magn. Magn. Mater.* *290*, 28–34.
- Ebeler, M., Pilgram, F., Wolz, K., Grim, G., and Franzreb, M. (2018). Magnetic Separation on a New Level: Characterization and Performance Prediction of a cGMP Compliant "Rotor-Stator" High-Gradient Magnetic Separator. *Biotechnol. J.* *13*, 1700448.
- Ebeler, M., Lind, O., Norrman, N., Palmgren, R., and Franzreb, M. (2018). One-step integrated clarification and purification of a monoclonal antibody using Protein A Mag Sepharose beads and a cGMP-compliant high-gradient magnetic separator. *N. Biotech.* *42*, 48–55.
- Brechmann, N.A., Eriksson, P.O., Eriksson, K., Oscarsson, S., Buijs, J., Shokri, A., Hjälm, G., and Chotteau, V. (2019). Pilot-scale process for magnetic bead purification of antibodies directly from non-clarified CHO cell culture. *Biotechnol. Prog.* *35*, e2775.
- Lind, O., Norrman, N., Häggblad Sahlberg, S., and Palmgren, R. (2022). A Method for Separating Biomolecules. Patent Nr. S2022229052. P.a.T. Office.
- Hagner-McWhirter, Å., Laurin, Y., Larsson, A., Bjerneld, E.J., and Rönn, O. (2015). Cy5 total protein normalization in Western blot analysis. *Anal. Biochem.* *486*, 54–61.
- Jay, F.T., Laughlin, C.A., and Carter, B.J. (1981). Eukaryotic translational control: adeno-associated virus protein synthesis is affected by a mutation in the adenovirus DNA-binding protein. *Proc. Natl. Acad. Sci. USA* *78*, 2927–2931.
- Liu, W., Liu, H., Wang, Y., Zhang, L., Wang, C., Li, H., Fan, X., Liang, Y., Peng, X., Xian, M., et al. (2019). Reduction of chromatin heteroaggregates by acid precipitation of mammalian cell culture and ramification in protein A chromatography for recombinant immunoglobulin G purification. *Mol. Cell. Biochem.* *450*, 65–73.
- Patrício, M.L., Cox, C.I., Blue, C., Barnard, A.R., Martinez-Fernandez de la Camara, C., and MacLaren, R.E. (2020). Inclusion of PF68 Surfactant Improves Stability of rAAV Titer when Passed through a Surgical Device Used in Retinal Gene Therapy. *Mol. Ther. Methods Clin. Dev.* *17*, 99–106.

35. Dickerson, R., Argento, C., Pieracci, J., and Bakhshayeshi, M. (2021). Separating Empty and Full Recombinant Adeno-Associated Virus Particles Using Isocratic Anion Exchange Chromatography. *Biotechnol. J.* 16, e2000015.
36. Hagner-McWhirter, Å. (2021). From cells to purified capsids: How to develop a scalable rAAV process. *Cell Gene Ther. Insights* 8, 611–619.
37. Cytiva (2023). Adeno-associated virus production in suspension HEK293 cells with single-use bioreactors. Application Note. <https://www.cytivalifesciences.com/en/us/solutions/cell-therapy/knowledge-center/resources/aav-vector-production-from-suspension-cells-to-bioreactors>.
38. Armbruster, D.A., and Pry, T. (2008). Limit of Blank, Limit of Detection and Limit of Quantitation. *Clin. Biochem. Rev.* 29, 49–52.